bioRxiv preprint doi: https://doi.org/10.1101/2021.09.10.459757; this version posted September 10, 2021. The copyright holder for this preprint (which was not certified by peer review) is the author/funder. All rights reserved. No reuse allowed without permission.

K_v1.3 induced hyperpolarisation and Ca_v3.2-mediated calcium entry are required for efficient Kaposi's sarcoma-associated herpesvirus lytic replication

Holli Carden[1], Mark L. Dallas[2], David J. Hughes[3], Jonathan D. Lippiat[4], Jamel Mankouri[1,*] & Adrian Whitehouse[1,5,*]

[1]*School of Molecular and Cellular Biology and Astbury Centre for Structural Molecular Biology, University of Leeds, Leeds, LS2 9JT, United Kingdom*

[2]*School of Pharmacy, University of Reading, Reading RG6 6AP, United Kingdom*

[3]*Biomedical Sciences Research Complex, School of Biology, University of St Andrews, North Haugh, St Andrews, KY16 9ST*

[4]*School of Biomedical Sciences, Faculty of Biological Sciences, University of Leeds, Leeds, LS2 9JT, United Kingdom*

[5]*Department of Biochemistry and Microbiology, Rhodes University, Grahamstown 6140, South Africa*

*Correspondence: Adrian Whitehouse, a.whitehouse@leeds.ac.uk Tel: +44 (0)113 343 7096 and Jamel Mankouri, j.mankouri:leeds.ac.uk Tel: +44 (0)113 343 5646

Running Title: K_v1.3 and Ca_v3.2 are required for KSHV reactivation

Keywords:

Kaposi's sarcoma (KS)-associated herpesvirus; antiviral; ion channel; K_v1.3; Ca_v3.2; NFAT; lytic replication.

bioRxiv preprint doi: https://doi.org/10.1101/2021.09.10.459757; this version posted September 10, 2021. The copyright holder for this preprint (which was not certified by peer review) is the author/funder. All rights reserved. No reuse allowed without permission.

Abstract

Understanding the host factors critical for Kaposi's sarcoma-associated herpesvirus (KSHV) lytic replication can identify new targets for therapeutic intervention. Using pharmacological and genetic silencing approaches, we reveal for the first time that KSHV requires a B cell expressed voltage-gated K^+ channel, $K_v1.3$, to enhance lytic replication. We show that the KSHV replication and transcription activator (RTA) protein upregulates $K_v1.3$ expression, leading to enhanced K^+ channel activity and hyperpolarisation of the B cell membrane. Enhanced $K_v1.3$ activity then promotes intracellular Ca^{2+} influx through $Ca_v3.2$, a T-type Ca^{2+} channel, leading to the Ca^{2+} driven nuclear localisation of NFAT and the subsequent NFAT1-responsive gene expression. Importantly, KSHV lytic replication and infectious virion production could be inhibited by both $K_v1.3$ and $Ca_v3.2$ blockers or through $K_v1.3$ silencing. These findings provide new mechanistic insight into the essential role of host ion channels during KSHV infection and highlight $K_v1.3$ and $Ca_v3.2$ as new druggable host factors that are key to the successful completion of KSHV lytic replication.

bioRxiv preprint doi: https://doi.org/10.1101/2021.09.10.459757; this version posted September 10, 2021. The copyright holder for this preprint (which was not certified by peer review) is the author/funder. All rights reserved. No reuse allowed without permission.

Introduction

Kaposi's sarcoma-associated herpesvirus (KSHV) is a gamma 2-herpesvirus directly linked to the development of Kaposi's sarcoma (KS), a highly vascular tumour of endothelial lymphatic origin, and several other AIDs-associated malignancies including primary effusion lymphoma (PEL) and some forms of multicentric Castleman's disease (MCD)[1-4]. KSHV exhibits a biphasic life cycle consisting of latent persistence or lytic replication. In contrast to other oncogenic herpesviruses in which latent gene expression drives tumorigenesis, both the latent and lytic replication phases are essential for KSHV-mediated tumorigenicity[5]. Latency is established in B cells and in the tumour setting, where viral gene expression is limited to the latency-associated nuclear antigen (LANA), viral FLICE inhibitory protein, viral cyclin, kaposins and several virally-encoded miRNAs[6-8]. Upon reactivation, KSHV enters the lytic replication phase, leading to the highly orchestrated expression of more than 80 viral proteins that are sufficient for the production of infectious virions[9,10]. In KS lesions, most infected cells harbour the virus in a latent state. However, a small proportion of cells undergo lytic replication that leads to the secretion of angiogenic, inflammatory and proliferative factors that act in a paracrine manner on latently-infected cells to enhance tumorigenesis[11]. Lytic replication also enhances genomic instability[12] and sustains KSHV episomes in latently-infected cells that would otherwise be lost during cell division[13]. The ability to inhibit the lytic replication phase therefore represents a therapeutic intervention strategy for the treatment of KSHV-associated diseases[14,15].

The transition from latent infection to lytic replication is controlled by both host and viral factors[16,17]. These factors converge on the regulation of the latency associated nuclear antigen (LANA) and the master regulator of the latent-lytic switch, KSHV replication and transcription activator (RTA) protein[18]. Notably, agents that mobilize intracellular Ca^{2+} can induce the expression of KSHV-RTA and enhance KSHV reactivation and lytic replication[19], however this activity can be blocked with inhibitors of calcineurin-dependent signal transduction[20]. Cytoplasmic concentrations of Ca^{2+} are regulated by a network of ion channels and transporters[21] . Ion channels are multi-subunit, pore-forming membrane proteins that control the rapid and selective passage of ions across the plasma membrane and the membranes of subcellular organelles[22]. As such, ion channels have a wide variety of roles in controlling the ion homeostasis of the cell and its organelles, action potential firing, membrane potential and cell volume. Given this wide range of functions and their ubiquitous nature, dysregulation of ion channels have been implicated in a variety of disorders and diseases known as channelopathies[23] and may also play an important role in enhancing cell proliferation and invasion of tumour cells.

bioRxiv preprint doi: https://doi.org/10.1101/2021.09.10.459757; this version posted September 10, 2021. The copyright holder for this preprint (which was not certified by peer review) is the author/funder. All rights reserved. No reuse allowed without permission.

Several stages of virus replication cycles, including virion entry, virus egress and the maintenance of an environment conducive to virus replication are in-part, dependent on the ability of virus proteins to manipulate ion channel activity[23,24]. Most notably, the pharmacological modulation of virus-targeted ion channels has been shown to impede virus replication, highlighting ion channels as promising candidates for host targeted anti-viral therapeutics. A catalogue of ion channel-blocking drugs have also been shown to possess antiviral activity, some of which are in widespread human use for ion channel-related diseases, highlighting new potential for drug repurposing. Amongst herpesviruses, varicella-zoster virus and herpes simplex virus have been shown to activate voltage-gated Na^+ channels and voltage-gated Ca^{2+} channels[25,26]. However, a specific role for host cell ion channels during the lytic replication stage of KSHV or any herpesvirus have yet to be fully defined. B lymphocytes, the primary site of KSHV latent infection, are regulated by a network of transporters and ion channels that control the cytoplasmic concentrations of calcium (Ca^{2+}), magnesium (Mg^{2+}) and zinc (Zn^{2+}), which act as important second messengers to regulate critical B cell effector functions[27]. The repertoire of ion channels in B cells include potassium (K^+) channels, Ca^{2+} channels, P2X receptors and transient receptor potential (TRP) channels, in addition to Mg^{2+} and Zn^{2+} transporters. To-date, a role for these channels during KSHV infection has not been described.

Here, we performed a systematic analysis of the role of host ion channels during the KSHV lytic replication phase in human B cells to reveal new avenues for host-directed therapeutic intervention. Using a combination of electrophysiological and biochemical approaches, we show that KSHV activates a voltage-gated K^+ channel $K_v1.3$, the pharmacological and genetic silencing of which inhibits KSHV lytic replication. We further define the mechanism for this dependence by showing that $K_v1.3$ activation leads to hyperpolarisation induced Ca^{2+} influx through a T-type Ca^{2+} channel $Ca_v3.2$, which enhances the nuclear localisation of NFAT1, which in turn is required to drive virus replication. We therefore reveal for the first time the essential role of $K_v1.3$ and $Ca_v3.2$ channels in the lytic replication cycle of a herpesvirus.

bioRxiv preprint doi: https://doi.org/10.1101/2021.09.10.459757; this version posted September 10, 2021. The copyright holder for this preprint (which was not certified by peer review) is the author/funder. All rights reserved. No reuse allowed without permission.

Material and Methods

Cell culture, antibodies and reagents

TREx-BCBL-1-RTA cells (kindly provided by Prof. Jae Jung, University of Southern California) are a BCBL-1-based primary effusion lymphoma (PEL) B cell line engineered to express exogenous Myc-tagged RTA upon addition of doxycycline, triggering reactivation of the KSHV lytic cycle. A549 and HEK-293T cell lines were purchased from the American Type Culture Collection (ATCC). U87 cells (kindly provided by Prof. J. Ladbury, University of Leeds) are a human brain glioblastoma astrocytoma cell line. A549, U87 and HEK-293T cells were grown in DMEM (Life Technologies) supplemented with 10% foetal calf serum (FCS) (Life Technologies) and 1% penicillin/streptomycin (P/S). TREx BCBL1-RTA cells were grown in RPMI 1640 medium (Life Technologies) supplemented with 10% FCS and 1% P/S, and maintained under hygromycin B (Life Technologies) selection (100 µg/ml). Reactivation into the lytic cycle was induced using 2 µg/ml doxycycline hyclate (Sigma) as previously described[28]. All cells were maintained at 37°C in a humidified incubator with 5% CO_2. pEGFP-N1 was obtained from Clontech, pRTA-EGFP and pORF57-GFP have been described previously[29-31]. Rabbit antibodies anti-Sp1 (EPR22648-50), anti-Lamin B1 and anti-NFAT1 were purchased from Abcam. Mouse monoclonal antibodies to GAPDH (1E6D9) and KSHV ORF57 (207.6) were obtained from Proteintech and Santa Cruz, respectively. Mouse monoclonal anti-c-Myc (9E10) and rabbit polyclonal anti-K_v1.3 antibodies were obtained from Sigma. KSHV ORF59 and KSHVGFP ORF65 were kind gifts from Prof. Britt Glaunsinger (University of California, Berkeley) and Prof. Shou-Jiang Gao (University of Pittsburgh), respectively.

(2R/S)-6-prenylnaringenin, Blood Depressing Substance I and ShK-Dap[22] were obtained from Bio-Techne. Mibefradil and pimozide were purchased from Cambridge Bioscience. 4-aminopyridine, calcium ionophore A23187, charybdotoxin, margatoxin, nifedipine, quinine hydrochloride dihydrate, SKF-96365, tetraethylammonium chloride and TRAM-34 were obtained from Sigma-Aldrich. Flunarizine, Cyclosporin A, Mithramycin A and KCl were purchased from Alfa Aesar, Fluorochem Limited, Insight Biotechnology and ThermoFisher, respectively. Human foetal brain (HFB) cDNA library was purchased from Invitrogen. Oligonucleotide primer sequences are available upon request. All primers were purchased from Sigma (UK).

Lentivirus-based shRNA Knockdown

Lentiviruses were generated by transfection of HEK-293T cells seeded in 12-well plates using a three-plasmid system, as previously described[28]. Per 6-well, 4 µl of lipofectamine 2000 (Thermo Scientific) were used together with 1 µg of pLKO.1 plasmid expressing shRNA against the protein of interest

bioRxiv preprint doi: https://doi.org/10.1101/2021.09.10.459757; this version posted September 10, 2021. The copyright holder for this preprint (which was not certified by peer review) is the author/funder. All rights reserved. No reuse allowed without permission.

(Dharmacon), 0.65 µg of pVSV.G, and 0.65 µg psPAX2. pVSV.G and psPAX2 were a gift from Dr. Edwin Chen (University of Westminster, London). Eight hours post-transfection, media was changed with 2 mL of DMEM supplemented with 10% (v/v) FCS. 500,000 TREx BCBL1-Rta cells in 6 well plates were infected by spin inoculation with the filtered viral supernatant for 60 min at 800 x g at room temperature, in the presence of 8 µg/mL of polybrene (Merck Millipore). Virus supernatants were removed 7 h post-spin inoculation and cells were maintained in fresh growth medium for 48 h prior to selection in 3 µg/mL puromycin (Sigma-Aldrich). Stable cell lines were generated after 8 days of selection.

Transient Transfections

Plasmid transfections were performed using Lipofectamine 2000 (Life Technologies), at a ratio of 2 ug plasmid to 1 ul Lipofectamine in 100 ul opti-MEM. Transfection media was incubated at room temperature for 15 minutes before 1x 10^6 cells were treated, dropwise. Cells were harvested after 24 hours.

Immunofluorescence

Cells were cultured overnight on poly-L-lysine (Life Technologies) coated glass coverslips in 24-well plates. Cells were fixed with 4% paraformaldehyde (Calbiochem) for 10 min and permeabilised with 0.1% Triton X-100 for 20 min as previously described[32]. Cells were blocked in PBS containing 1% BSA for 1 h at 37°C and labelled with primary antibodies for 1 h at 37°C. Cells were washed five times with PBS and labelled with appropriate secondary antibodies for 1 h at 37°C. Cells were washed five times with PBS and mounted in VECTASHIELD containing DAPI (Vector Labs). Images were obtained using a Zeiss LSM700 Inverted Microscope confocal microscope and processed using ZEN 2009 imaging software (Carl Zeiss) as previously described[29].

Electrophysiology

TREx BCBL1-RTA cells seeded onto poly-L-lysine (Life Technologies) coated glass coverslips and were transferred to a recording chamber, containing 140 mM NaCl, 5 mM KCl, 2 mM $MgCl_2$, 10 mM HEPES-NaOH, pH 7.2, 2 mM $CaCl_2$, 10 mM glucose, and mounted on the stage of a Nikon Eclipse inverted microscope. Patch pipettes (5–8 MΩ) were filled with a solution consisting of: 140 mM KCl, 5 mM EGTA, 2 mM $MgCl_2$, 1 mM $CaCl_2$, 10 mM HEPES KOH, pH 7.2, 10 mM glucose. Voltage-clamp recordings were performed using a HEKA EPC-10 integrated patch clamp amplifier controlled by Patchmaster software (HEKA). Series resistance was monitored after breaking into the whole cell configuration. To examine K^+ currents, a series of depolarizing steps were performed from −100 to +60 mV in 10 mV

bioRxiv preprint doi: https://doi.org/10.1101/2021.09.10.459757; this version posted September 10, 2021. The copyright holder for this preprint (which was not certified by peer review) is the author/funder. All rights reserved. No reuse allowed without permission.

increments for 100 ms. Resting membrane potential was measured using the current clamp mode of the amplifier. Results are shown as the mean ± SEM of n number of individual cells. Statistical analysis was performed using an unpaired Student's T test. $p<0.05$ was considered statistically significant.

Flow Cytometry

Bis-(1,3-Dibutylbarbituric Acid) Trimethine Oxonol ($DiBAC_4(3)$) and Fura Red (both ThermoFisher) were added to cells at a final concentration of 1 µM in RPMI-media. Cells were incubated at 37°C with Fura Red for 30 min or $DiBAC_4(3)$ for 5 min and washed in PBS. Cells were analysed on a CytoFLEX Flow Cytometer (Beckman). Data were quantified using FlowJo software as previously described[33] (Tree Star, Ashland, OR, USA).

Proliferation (MTS) assays

Cellular viability was determined using non-radioactive CellTiter 96 AQueous One Solution Cell Proliferation Assay (MTS) reagent (Promega), according to the manufacturer's recommendations[29]. Briefly, TREx BCBL1-RTA cells (~20,000) were seeded in triplicate in a flat 96-well tissue culture plates (Corning) and treated with the indicated inhibitors for 24 h. CellTiter 96 AQueous One Solution Reagent was added to the cells for 1 h at 5% CO_2, 37^{O}C. Absorbances were measured at 490 nm using an Infinite plate reader (Tecan).

Two-step quantitative reverse transcription PCR (qRT-PCR)

Total RNA was extracted using the Monarch® Total RNA Miniprep Kit (New England Biolabs) as per the manufacturer's protocol. RNA (1 µg) was diluted in a total volume of 16 µl nuclease-free water, and 4 µl LunaScript RT SuperMix (5X) (New England Biolabs) was added to each sample. Reverse transcription was performed using the protocol provided by the manufacturer. cDNA was stored at -20°C, RNA was stored at -80°C. Quantitative PCR (qPCR) reactions (20 µl) included 1X SensiMix SYBR green master mix (Bioline), 0.5 µM of each primer and 5 µl template cDNA (used at 1:200 dilution in RNase-free water). Cycling was performed in a RotorGene Q instrument (Qiagen), using a previously described cycling programme[29]. Relative gene expression was calculated using the ΔΔCT method, as previously described[29]. Statistical significance was validated using a Student's t-test.

Chromatin immunoprecipitation (ChIP)

Formaldehyde-crosslinked chromatin was prepared using the Pierce Chromatin Prep Module (Thermo Scientific) following the manufacturer's protocol. Cells (2×10^6) were digested with six units of micrococcal nuclease (MNase) per 100 µl of MNase Digestion buffer in a 37°C water bath for 15 min.

bioRxiv preprint doi: https://doi.org/10.1101/2021.09.10.459757; this version posted September 10, 2021. The copyright holder for this preprint (which was not certified by peer review) is the author/funder. All rights reserved. No reuse allowed without permission.

These conditions resulted in optimal sheared chromatin with most fragments ranging from 150–300 base pairs in size. Immunoprecipitations were performed using EZ-ChIP kit (Millipore) kits overnight at 4°C and contained 50 µl of digested chromatin (2 x 10^6 cells), 450 µl of ChIP dilution buffer and 1.5 µg of RNAPII antibody (clone CTD4H8) (Millipore) or isotype antibody, normal mouse IgG (Millipore). qPCR reactions were performed using either 2 µl of immunoprecipitated DNA or 2 µl of input DNA as template.

Immunoblotting

Protein samples were separated on SDS-PAGE gels as previously described[34], and transferred to nitrocellulose membranes (Amersham) via semi-dry transfer using a Trans-Blot® Turbo™ blotter (BioRad). Membranes were blocked in TBS + 0.1% Tween 20 and 5% dried skimmed milk powder and probed with relevant primary antibodies followed by horseradish peroxidase (HRP)-conjugated polyclonal goat anti-mouse and polyclonal goat anti-rabbit secondary antibodies (Dako). Membranes were treated with EZ-ECL (Geneflow) and imaged using a G-Box (Syngene).

bioRxiv preprint doi: https://doi.org/10.1101/2021.09.10.459757; this version posted September 10, 2021. The copyright holder for this preprint (which was not certified by peer review) is the author/funder. All rights reserved. No reuse allowed without permission.

Results

K^+ channels are required for efficient KSHV reactivation

K^+ channels represent the largest family of ion channels with over 70 genes identified in the human genome[35]. We first sought to determine if their activity is required for efficient KSHV lytic replication. Here virus reactivation assays were performed in the presence of potassium chloride (KCl) to collapse cellular K^+ channel gradients, or the broad spectrum K^+ channel blockers, barium chloride ($BaCl_2$), tetraethylammonium (TEA) and quinidine (Qn). All were assessed at non-toxic concentrations (Supp Fig 1). KSHV reactivation was assessed in TREx BCBL1-RTA cells, a latently infected KSHV B-lymphocyte cell line that express a Myc-tagged viral RTA under the control of a doxycycline-inducible promoter. Upon analysis, TREx BCBL1-RTA cells reactivated for 24 h in the presence of each K^+ channel inhibitor showed a drastic reduction in the expression early ORF57, delayed early ORF59 and the late minor capsid (mCapsid) ORF65 proteins (**Fig 1a**). No such reduction was observed in the expression of Myc-RTA or GAPDH, highlighting specific effects on lytic replication as opposed to dox-induced RTA induction. These data indicate a requirement for K^+ channel function during the KSHV lytic replicative cycle.

We next investigated the molecular identity of the specific K^+ channel(s) required for KSHV lytic replication to reveal more specific drug targets. K^+ channels can be divided into subfamilies of voltage-gated K^+ channels (K_v), calcium-activated K^+ channels (K_{Ca}), inwardly rectifying K^+ channels (K_{ir}) and two-pore domain K+ channels (K2P) channels. We found that treatment with 4-aminopyridine (4-AP), a non-selective K_v blocker, led to a concentration-dependent reduction in lytic replication (**Fig 1b**), suggestive of a role for K_v channels during lytic induction. Electrophysiological studies have identified an array of functional K_v channels expressed within B lymphocytes, with a member of the *Shaker* related family, $K_v1.3$, most extensively characterised[36]. When specific $K_v1.3$ blockers margatoxin (MgTX) and ShK-Dap[22] were included in our reactivation assays, a concentration-dependent reduction of lytic gene expression was observed, implicating a role for this channel during lytic KSHV replication (**Fig 1c-d**). In contrast, TRAM-34, a blocker of B lymphocyte $K_{Ca}3.1$ channels, showed no effect on lytic KSHV protein production (**Fig 1e**).

To confirm a role for $K_v1.3$ during KSHV lytic replication, TREx BCBL1-RTA cells were transduced with lentivirus-based shRNAs to effectively deplete $K_v1.3$ by over 85% (**Fig 2a-b**). Reactivation assays showed that $K_v1.3$ silencing led to a significant reduction in ORF57, ORF59 and ORF65 proteins

bioRxiv preprint doi: https://doi.org/10.1101/2021.09.10.459757; this version posted September 10, 2021. The copyright holder for this preprint (which was not certified by peer review) is the author/funder. All rights reserved. No reuse allowed without permission.

compared to scrambled controls (**Fig 2c**). To examine whether the depletion of $K_v1.3$ also influenced infectious virus production, supernatants of reactivated TREx BCBL1-RTA cells were used to re-infect naive cells and KSHV infection was determined by qRT-PCR. Cells reinfected with supernatants from $K_v1.3$ depleted cells showed a ~85% reduction in viral mRNA compared to control cells (**Fig. 2d**). Together, these data confirmed that KSHV requires the function of B cell $K_v1.3$ channels to undergo efficient lytic replication and infectious virus production.

KSHV enhances $K_v1.3$ expression and activity

As KSHV is dependent on $K_v1.3$ to complete its lytic replication cycle, its ability to modulate $K_v1.3$ activity was next investigated. qRT-PCR and immunoblotting analysis showed that $K_v1.3$ expression increased in TREx BCBL1-RTA cells undergoing lytic replication compared to latent cells (**Fig. 3a**). To elucidate whether the increase in $K_v1.3$ expression led to enhanced K^+ efflux mediated by $K_v1.3$ channels during lytic replication, whole-cell patch clamp analysis was performed. Electrophysiological recordings revealed a voltage-gated outward K^+ current present in latent TREx BCBL1-RTA cells that was significantly enhanced in cells undergoing lytic replication (**Fig. 3b**). To conclusively determine that $K_v1.3$ channels were responsible for these changes, recordings were repeated in the presence of ShK-Dap[22], which led to a dramatic inhibition of the K^+ current (**Fig. 3b**). A similar reduction was observed in cells depleted for $K_v1.3$ using lentivirus-based shRNAs, compared to scrambled controls (**Fig 3c**). Notably, we also observed that reactivated TREx BCBL1-RTA cells exhibited a significantly more hyperpolarised membrane compared to latent cells (**Fig. 3d**), which was reversed upon $K_v1.3$ depletion (**Fig. 3e**). Membrane hyperpolarisation was also confirmed using a membrane potential-sensitive dye, bis (1,3-dibutylbarbituric acid) trimethine oxonol; $DiBAC_4(3)$. Results showed a time-dependent decrease in fluorescence intensity in lytic cells, consistent with enhanced membrane hyperpolarization (**Fig 3e**). In contrast, addition of the calcium ionophore A23187, which induces depolarisation, enhanced DiBAC4(3) fluorescence. Moreover, no reduction in DiBAC4(3) fluorescence was observed in $K_v1.3$ depleted cells (**Fig 3f**). Together these results demonstrate that KSHV lytic replication increases $K_v1.3$ expression, resulting in an enhanced $K_v1.3$ currents and hyperpolarisation during lytic KSHV replication.

KSHV RTA mediates the upregulation of $K_v1.3$ during lytic replication

We next investigated the mechanism by which KSHV enhances $K_v1.3$ currents. Given that membrane hyperpolarisation was observed as early as 4 h post-reactivation, we examined whether the KSHV

bioRxiv preprint doi: https://doi.org/10.1101/2021.09.10.459757; this version posted September 10, 2021. The copyright holder for this preprint (which was not certified by peer review) is the author/funder. All rights reserved. No reuse allowed without permission.

early proteins were sufficient to induce $K_v1.3$ expression and activation. A549 and U87 cells were transiently transfected with control GFP, RTA-GFP or ORF57-GFP expression constructs and $K_v1.3$ transcript levels were assessed by qRT-PCR at 24 h post-transfection. We found that RTA-GFP alone was sufficient to induce $K_v1.3$ expression at the transcript level (**Fig 4a-b**), confirming KSHV RTA transcriptional activator as the direct inducer of $K_v1.3$ expression.

Specificity Protein (Sp) 1 functions as a co-adapter for RTA-mediated transactivation and has been shown to regulate $K_v1.3$ expression[37]. To further dissect the relationship between KSHV-RTA and $K_v1.3$, we examined a potential cooperative role for Sp1 during the upregulation of $K_v1.3$ during lytic replication. RTA-GFP transfections were performed in the presence of Mithramycin A, a selective Sp1 inhibitor that displaces Sp1 binding from its target promoter[38]. Results showed Mithramycin A treatment supressed the RTA-mediated increase in $K_v1.3$ expression (**Fig 4c**), but had little effect on the RTA-mediated upregulation of the IL-6 promoter, suggestive of an in-direct mechanism whereby Sp1 recruits RTA to the $K_v1.3$ promoter. ChIP assays further confirmed an association of both RTA and Sp1 with the $K_v1.3$ promoter, which significantly increased during lytic replication (**Fig 4d**). Together, these data reveal KSHV RTA as the key driver of $K_v1.3$ expression during the KSHV lytic cycle.

$K_v1.3$ induced membrane hyperpolarisation provides the driving force for Ca^{2+} influx required for KSHV reactivation

In B lymphocytes, $K_v1.3$ maintains a hyperpolarised membrane potential that is necessary to sustain the driving force for Ca^{2+} entry. $K_v1.3$ therefore indirectly modulates an array of Ca^{2+}-dependent cellular processes in B cells. To assess the role of $K_v1.3$ during lytic replication, we assayed Ca^{2+} influx into TREx BCBL1-RTA cells during the KSHV lytic cycle using the ratiometric Ca^{2+} dye Fura-Red and flow cytometry analysis. We observed an increase in cytoplasmic Ca^{2+} over a 24 h period of lytic reactivation (**Fig 5a**), that was absent in $K_v1.3$-depleted TREx BCBL1-RTA cells compared to scrambled controls (**Fig. 5b**). Based on these data, we investigated whether Ca^{2+} influx defines the requirement of $K_v1.3$ for efficient lytic replication. TREx BCBL1-RTA cells were reactivated in the absence or presence of the Ca^{2+} ionophore A23187, which led to enhanced lytic ORF57 protein levels compared to control cells (**Fig. 5c)**. We next determined whether A23187 had the ability to recover KSHV lytic replication in a $K_v1.3$ depleted cell line. Notably, lytic ORF57 protein production was observed in $K_v1.3$ silenced cells, suggesting that A23187 could override the dependence of KSHV on $K_v1.3$ (**Fig 5d**). Together, these data suggest that Ca^{2+} influx is essential for efficient KSHV lytic replication and is induced by $K_v1.3$-mediated hyperpolarisation.

bioRxiv preprint doi: https://doi.org/10.1101/2021.09.10.459757; this version posted September 10, 2021. The copyright holder for this preprint (which was not certified by peer review) is the author/funder. All rights reserved. No reuse allowed without permission.

KSHV-mediated Ca^{2+} influx requires the T-type voltage-gated calcium channel, $Ca_v3.2$

We next sought to identify the Ca^{2+} channel(s) required for KSHV-mediated Ca^{2+} influx. Here KSHV lytic replication was assessed in presence of specific Ca^{2+} channel modulating drugs at non-cytotoxic concentations, to identify candidate Ca^{2+} channel members (**Supp Fig 1**). Results showed that SKF-96365, an inhibitor of TRP channels and STIM1, and T-type calcium channel blocking drugs dramatically reduced the levels of KSHV lytic replication (**Fig 6ai**). In contrast, Nifedipine, an L-type voltage-gated Ca^{2+} channel inhibitor had no significant effect on KSHV lytic replication (**Fig 6aii**). Additional reactivation assays performed in the presence of Mibefradil reinforced the requirement of T-type voltage-gated Ca^{2+} channels for KSHV lytic replication (**Fig 6aiii**).

In humans, the expression of the three T-type Ca^{2+} channels, namely $Ca_v3.1$, $Ca_v3.2$ and $Ca_v3.3$, are cell type dependent[39]. We therefore performed qRT-PCR analysis to confirm the expression profiles of each channel in TREx BCBL1-RTA cells. Human foetal brain (HFB) cDNA was included in this analysis as a positive control for all three $Ca_v3.x$ channel types. Analysis showed that $Ca_v3.2$ is the only T-type Ca^{2+} channel expressed in TREx BCBL1-RTA cells (**Fig 6b**). To verify a role for $Ca_v3.2$ during KSHV-mediated Ca^{2+} influx, KSHV lytic replication was monitored in the presence of (2R/S)-6-prenylnaringenin (PNG), a specific $Ca_v3.2$ blocker[40]. The results showed a dramatic reduction of ORF57 expression, an indicator of KSHV lytic replication implicating a role for this channel during lytic KSHV replication. This was reinforced by results showing that the PNG-mediated inhibition could be rescued upon the addition of A23187 (**Fig 6c**). Together, these data reveal the requirement for $Ca_v3.2$-mediated Ca^{2+} influx for efficient KSHV lytic replication in response to $K_v1.3$-mediated hyperpolarisation.

KSHV-mediated Ca^{2+} influx initiates NFAT1 nuclear localisation and NFAT1-mediated gene expression

Ca^{2+} influx can initiate multiple signalling pathways, including the serine/threonine phosphatase calcineurin and its target transcription factor NFAT (nuclear factor of activated T cells)[21]. The phosphatase activity of calcineurin is activated through binding of the Ca^{2+}-calmodulin complex, displacing the calcineurin autoinhibitory domain from the active site of the enzyme. Dephosphorylation of cytoplasmic NFAT proteins by calcineurin unmasks their nuclear localization sequences, leading to nuclear translocation and NFAT-responsive gene expression. To investigate whether KSHV-mediated hyperpolarisation and Ca^{2+} influx promote the nuclear translocation of NFAT,

bioRxiv preprint doi: https://doi.org/10.1101/2021.09.10.459757; this version posted September 10, 2021. The copyright holder for this preprint (which was not certified by peer review) is the author/funder. All rights reserved. No reuse allowed without permission.

its nuclear/cytoplasmic distribution was compared in latent versus lytic TREx BCBL1-RTA cells using immunofluorescence analysis. Results showed that NFAT1 translocates to the nucleus in lytic cells, but remains cytoplasmic during latent infection (**Fig. 7a**). This result was confirmed by immunoblot analysis of subcellular fractions of latent and lytic TREx BCBL1-RTA cells (**Fig. 7b**). The nuclear localisation of NFAT was found to be dependent on both $K_v1.3$-mediated hyperpolarisation and $Ca_v3.2$-dependent Ca^{2+} influx, as it was prevented by both ShK-Dap^{22} and PNG treatment (**Fig 7a**). The nuclear localisation of NFAT1 in lytic cells was also shown to require calcineurin activity, since it was inhibited in the presence of the calcineurin inhibitor, cyclosporin A (CsA) (**Fig. 7a**). Consistent with the enhanced nuclear localisation of NFAT, we observed an increase in NFAT-responsive gene expression during KSHV lytic replication, which was reduced in the presence of ShK-Dap^{22}, PNG (**Fig. 7c**), and upon $K_v1.3$ depletion (**Fig. 7d**). Together, these data suggest that the KSHV-induced hyperpolarisation mediated by $K_v1.3$ and the subsequent influx of Ca^{2+} through $Ca_v3.2$, enhances the nuclear localisation of NFAT1 and induces NFAT-driven gene expression.

bioRxiv preprint doi: https://doi.org/10.1101/2021.09.10.459757; this version posted September 10, 2021. The copyright holder for this preprint (which was not certified by peer review) is the author/funder. All rights reserved. No reuse allowed without permission.

Discussion

KSHV infection is responsible for various malignancies, including KS, PEL and some cases of MCD. These diseases are highly associated with compromised immune function, and as such represent some of the most common cancers in areas of the world where HIV infection is prevalent[1]. Notably, KS is the most common cancer in many sub-Saharan countries. Therefore, understanding the molecular mechanisms that underlie KSHV biology is of the utmost importance if developing targeted therapeutic approaches. KSHV latency-associated viral proteins have been well characterised in transformation and tumourigenesis pathways; however, it is clear that KSHV also requires the lytic phase to drive tumourigenesis[14]. This is supported by a number of studies showing abrogation of KSHV gene expression impairs KSHV-associated oncogenesis. This is also emphasised by successful treatment of KS patients with drugs that inhibit KSHV replication indicate that the lytic phase is required for both the initiation of KS and the maintenance of disease[41]. Lytic genes encode angiogenic and KS growth factors which stimulate the proliferation of latently-infected cells and angiogenesis in a paracrine manner. Lytic replication can also replenish episomes lost within highly proliferating tumour cells, maintaining viral latency in select cell populations. Discovery of both the viral and cellular determinants that control lytic induction can therefore inform new therapeutic targets for anti-KSHV drug discovery. This is particularly important in light of the increasing number of AIDS-associated, Iatrogenic and classic KS cases[42] due to the increased survival rates of AIDS patients, the higher success rates of transplant surgery, and increasing global life expectancy[43].

Ion channels control a range of cellular processes that are known to be co-opted by viruses[23,24]. Accordingly, ion channels have emerged as druggable host targets to prevent both RNA and DNA viruses from the successful completion of their life cycles. Given the known dependence of KSHV lytic replication on Ca^{2+} signalling[20], coupled to previous studies demonstrating the ability of VZV and HSV-1 to activate Na^{+} and Ca^{2+} family members[25,26], we specifically investigated the role of B cell expressed ion channels during KSHV lytic reactivation. Using known pharmacological ion channel modulators, genetic silencing approaches and electrophysiological analysis, we reveal for the first time that KSHV requires a B-cell expressed voltage-gated K^{+} channel, $K_v1.3$, to enhance lytic replication. We show that the KSHV RTA protein upregulates $K_v1.3$ expression via indirect Sp1-mediated transactivation. Enhanced $K_v1.3$ expression and activity led to hyperpolarisation of the B-cell membrane potential, initiating Ca^{2+} influx through a T-type Ca^{2+} channel, $Ca_v3.2$. T-type Ca^{2+} channels undergo both voltage-dependent activation and inactivation, with $Ca_v3.2$ maximally inactivated at the depolarised membrane potentials that we measured from latently-infected cells[39]. The combination of reduced

bioRxiv preprint doi: https://doi.org/10.1101/2021.09.10.459757; this version posted September 10, 2021. The copyright holder for this preprint (which was not certified by peer review) is the author/funder. All rights reserved. No reuse allowed without permission.

inactivation and the increase in driving force on Ca^{2+} ions resulting from hyperpolarisation, enhances Ca^{2+} influx via these channels. This led to $Ca_v3.2$-mediated Ca^{2+} elevation and the subsequent Ca^{2+} driven nuclear localisation of NFAT1 to complete the KSHV lytic replication cycle. We therefore reveal the $K_v1.3$-$Ca_v3.2$ axis as a direct contributor to the lytic replication of KSHV in B cells (**Fig. 8**).

A striking feature of KSHV is the homology of its numerous ORFs to cellular genes[10]. These virus-encoded proteins contribute to KSHV-associated pathogenesis by subverting cell signalling pathways, including interferon-regulated anti-viral responses, cytokine-regulated cell growth, cell cycle progression and apoptosis. Many viruses encode viroporins[44]; ion channel proteins that modulate the ionic milieu of intracellular organelles to control virus protein stability and trafficking. However, no known viroporin exists amongst the ORFs of KSHV and it is therefore likely that evolution has tailor-made its proteins to regulate the expression of host cell ion channels to induce the Ca^{2+} signalling required for both latent and lytic replicative phases. Tumorigenesis may represent a by-product of this regulation, since in an array of human cancers, $K_v1.3$ expression is enhanced and correlates with the grade of tumour malignancy[45]. It is also noteworthy that features of KS tumours mirror the phenotypic effects of $K_v1.3$ overexpression, including the enhanced expression of inflammatory and angiogenic cytokines and uncontrolled cell cycle progression. This may reveal the KSHV driven activation of $K_v1.3$ as a channelopathy, a group of diseases characterised by altered function of ion channel proteins or their regulatory subunits. Several ion channel inhibitors specifically target $K_v1.3$, these inhibitors can either comprise small organic molecules such as quinine and 4AP or peptides purified from venom[37,46]. These venom-derived peptides are highly stable and resist denaturation due to the disulphide bridges formed within the molecules[46]. As with margatoxin, most are derived from scorpion venom, such as agitoxins, kaliotoxin, maurotoxin and noxiustoxin yet many inhibitors have been derived from ShK, a peptide originally isolated from the sea anemone *Stichodactyla helianthus*[47]. Given the abundance of natural sources for $K_v1.3$-inhibition a safe, effective therapeutic based on these compounds is a promising target for prevention. Additionally, it is interesting to note that the anti-CD20 monoclonal antibody rituximab, a known $K_v1.3$ inhibitor, substantially improves the outcome of KSHV patients[48]. $Ca_v3.2$ inhibitors, including mibefradil, are also FDA approved as anti-hypertensive agents[49], presenting additional opportunities for drug repurposing for the treatment of KSHV-associated diseases.

Finally, K_v channels have been previously identified as a restriction factor to the entry of both Hepatitis C virus[50] and Merkel cell polyomavirus[51], through their abilities to inhibit endosome acidification-mediated viral membrane fusion. Whilst the inhibition of endosomal acidification has been shown to

bioRxiv preprint doi: https://doi.org/10.1101/2021.09.10.459757; this version posted September 10, 2021. The copyright holder for this preprint (which was not certified by peer review) is the author/funder. All rights reserved. No reuse allowed without permission.

reduce the entry and trafficking of KSHV virions, our electrophysiological analysis revealed enhanced cell surface $K_v1.3$ activity during lytic replication that directly contributed to the hyperpolarised membrane potential of cells that was required for efficient KSHV replication. Thus, whilst additional roles of $K_v1.3$ in endosomes cannot be excluded, our data suggest a divergent role of $K_v1.3$ during herpesvirus infection that may be cell-type and/or virus specific.

In conclusion, we reveal the requirement of $K_v1.3$ and $Ca_v3.2$ for KSHV reactivation. To date, compounds targeting $K_v1.3$ are in preclinical development[52], whilst some $Ca_v3.2$ blockers are FDA approved as antihypertensives and antiarrhythmics[49]. Further studies targeting these channels in KSHV-associated diseases are now warranted, which may reveal these channels as a host-directed therapeutic prospect for anti-KSHV drug development.

Acknowledgements

This work was supported by a Rosetrees Trust PhD studentship, M662 (Whitehouse) and a Royal Society University Research Fellowship, G:480764 (Mankouri). We thank Professor Jae Jung, University of Southern California School of Medicine, Los Angeles, for the TREx BCBL1-RTA cells and Prof. J. Ladbury, University of Leeds for U87 cells and Dr Edwin Chen, University of Westminster for the lentivirus vectors. KSHV ORF59 and KSHV ORF65 antibodies were kind gifts from Prof. Britt Glaunsinger (University of California, Berkeley) and Prof. Shou-Jiang Gao (University of Pittsburgh), respectively.

bioRxiv preprint doi: https://doi.org/10.1101/2021.09.10.459757; this version posted September 10, 2021. The copyright holder for this preprint (which was not certified by peer review) is the author/funder. All rights reserved. No reuse allowed without permission.

References

1. Ganem, D. KSHV and the pathogenesis of Kaposi sarcoma: listening to human biology and medicine. *Journal of Clinical Investigation* **120**, 939-949 (2010).
2. Dittmer, D.P. & Damania, B. Kaposi's Sarcoma-Associated Herpesvirus (KSHV)-Associated Disease in the AIDS Patient: An Update. *Cancer Treat Res* **177**, 63-80 (2019).
3. Lange, P. & Damania, B. Kaposi Sarcoma-Associated Herpesvirus (KSHV). *Trends Microbiol* **28**, 236-237 (2020).
4. He, M.*, et al.* Molecular Biology of KSHV in Relation to HIV/AIDS-Associated Oncogenesis. *Cancer Treat Res* **177**, 23-62 (2019).
5. Giffin, L. & Damania, B. KSHV: pathways to tumorigenesis and persistent infection. *Adv Virus Res* **88**, 111-159 (2014).
6. Dittmer, D.*, et al.* A cluster of latently expressed genes in Kaposi's sarcoma-associated herpesvirus. *Journal of Virology* **72**, 8309-8315 (1998).
7. Staskus, K.A.*, et al.* Kaposi's sarcoma-associated herpesvirus gene expression in endothelial (spindle) tumor cells. *J Virol* **71**, 715-719 (1997).
8. McClure, L.V. & Sullivan, C.S. Kaposi's sarcoma herpes virus taps into a host microRNA regulatory network. *Cell Host Microbe* **3**, 1-3 (2008).
9. Broussard, G. & Damania, B. Regulation of KSHV Latency and Lytic Reactivation. *Viruses* **12**(2020).
10. Arias, C.*, et al.* KSHV 2.0: a comprehensive annotation of the Kaposi's sarcoma-associated herpesvirus genome using next-generation sequencing reveals novel genomic and functional features. *PLoS Pathog* **10**, e1003847 (2014).
11. Nicholas, J. Human herpesvirus 8-encoded proteins with potential roles in virus-associated neoplasia. *Frontiers in Bioscience* **12**, 265-281 (2007).
12. Jackson, B.R., Noerenberg, M. & Whitehouse, A. A Novel Mechanism Inducing Genome Instability in Kaposi's Sarcoma-Associated Herpesvirus Infected Cells. *PLoS Pathog* **10**, e1004098 (2014).
13. Grundhoff, A. & Ganem, D. Inefficient establishment of KSHV latency suggests an additional role for continued lytic replication in Kaposi sarcoma pathogenesis. *J Clin Invest* **113**, 124-136 (2004).
14. Manners, O., Murphy, J.C., Coleman, A., Hughes, D.J. & Whitehouse, A. Contribution of the KSHV and EBV lytic cycles to tumourigenesis. *Curr Opin Virol* **32**, 60-70 (2018).
15. Hughes, D.J., Wood, J.J., Jackson, B.R., Baquero-Perez, B. & Whitehouse, A. NEDDylation is essential for Kaposi's sarcoma-associated herpesvirus latency and lytic reactivation and represents a novel anti-KSHV target. *PLoS Pathog* **11**, e1004771 (2015).
16. Aneja, K.K. & Yuan, Y. Reactivation and Lytic Replication of Kaposi's Sarcoma-Associated Herpesvirus: An Update. *Front Microbiol* **8**, 613 (2017).
17. Lukac, D.M. & Yuan, Y. Reactivation and lytic replication of KSHV. in *Human Herpesviruses: Biology, Therapy, and Immunoprophylaxis* (eds. Arvin, A.*, et al.*) (Cambridge, 2007).
18. Purushothaman, P., Dabral, P., Gupta, N., Sarkar, R. & Verma, S.C. KSHV Genome Replication and Maintenance. *Front Microbiol* **7**, 54 (2016).
19. Chang, J., Renne, R., Dittmer, D. & Ganem, D. Inflammatory cytokines and the reactivation of Kaposi's sarcoma-associated herpesvirus lytic replication. *Virology* **266**, 17-25 (2000).
20. Zoeteweij, J.P.*, et al.* Targeted inhibition of calcineurin signaling blocks calcium-dependent reactivation of Kaposi sarcoma-associated herpesvirus. *Blood* **97**, 2374-2380 (2001).
21. Crabtree, G.R. & Schreiber, S.L. SnapShot: Ca2+-calcineurin-NFAT signaling. *Cell* **138**, 210-210.e211 (2009).

bioRxiv preprint doi: https://doi.org/10.1101/2021.09.10.459757; this version posted September 10, 2021. The copyright holder for this preprint (which was not certified by peer review) is the author/funder. All rights reserved. No reuse allowed without permission.

22. Brown, B., Nguyen, H. & Wulff, H. Recent advances in our understanding of the structure and function of more unusual cation channels [version 1; peer review: 2 approved]. *F1000Research* **8**(2019).
23. Charlton, F.W.*, et al.* Ion Channels as Therapeutic Targets for Viral Infections: Further Discoveries and Future Perspectives. LID - 10.3390/v12080844 [doi] LID - 844.
24. Hover, S., Foster, B., Barr, J.N. & Mankouri, J. Viral dependence on cellular ion channels - an emerging anti-viral target?
25. Kennedy, P.G.*, et al.* Varicella-zoster viruses associated with post-herpetic neuralgia induce sodium current density increases in the ND7-23 Nav-1.8 neuroblastoma cell line.
26. Ding, L.*, et al.* T-type calcium channels blockers inhibit HSV-2 infection at the late stage of genome replication.
27. Mahtani, T. & Treanor, B. Beyond the CRAC: Diversification of ion signaling in B cells. *Immunological Reviews* **291**, 104-122 (2019).
28. Baquero-Perez, B.A.-O.*, et al.* The Tudor SND1 protein is an m(6)A RNA reader essential for replication of Kaposi's sarcoma-associated herpesvirus. LID - 10.7554/eLife.47261 [doi] LID - e47261.
29. Baquero-Pérez, B. & Whitehouse, A. Hsp70 Isoforms Are Essential for the Formation of Kaposi's Sarcoma-Associated Herpesvirus Replication and Transcription Compartments. *PLOS Pathogens* **11**, e1005274 (2015).
30. Schumann, S.*, et al.* Targeting the ATP-dependent formation of herpesvirus ribonucleoprotein particle assembly as an antiviral approach.
31. Gould, F., Harrison, S.M., Hewitt, E.W. & Whitehouse, A. Kaposi's sarcoma-associated herpesvirus RTA promotes degradation of the Hey1 repressor protein through the ubiquitin proteasome pathway. *Journal of Virology* **83**, 6727-6738 (2009).
32. Calderwood, M.A., Hall, K.T., Matthews, D.A. & Whitehouse, A. The herpesvirus saimiri ORF73 gene product interacts with host-cell mitotic chromosomes and self-associates via its C terminus. *J Gen Virol* **85**, 147-153 (2004).
33. Nwogu, N.*, et al.* Cellular sheddases are induced by Merkel cell polyomavirus small tumour antigen to mediate cell dissociation and invasiveness. *PLoS Pathog* **14**, e1007276 (2018).
34. Whitehouse, A., Stevenson, A., Cooper, M. & Meredith, D. Identification of a cis-acting element within the herpesvirus saimiri ORF 6 promoter that is responsive to the HVS.R transactivator. *Journal of General Virology* **78**, 1411-2658 (1997).
35. Sansom, M.S.P.*, et al.* Potassium channels: structures, models, simulations. *Biochimica et Biophysica Acta (BBA) - Biomembranes* **1565**, 294-307 (2002).
36. Wulff, H., Knaus, H.-G., Pennington, M. & Chandy, K.G. K⁺ Channel Expression during B Cell Differentiation: Implications for Immunomodulation and Autoimmunity. *The Journal of Immunology* **173**, 776 (2004).
37. Jang, S.H.*, et al.* Nuclear localization and functional characteristics of voltage-gated potassium channel Kv1.3. *J Biol Chem* **290**, 12547-12557 (2015).
38. Liu, R.*, et al.* Mithramycin A suppresses basal triple-negative breast cancer cell survival partially via down-regulating Krüppel-like factor 5 transcription by Sp1. *Scientific Reports* **8**, 1138 (2018).
39. Perez-Reyes, E. Molecular physiology of low-voltage-activated t-type calcium channels.
40. Sekiguchi, F.*, et al.* Blockade of T-type calcium channels by 6-prenylnaringenin, a hop component, alleviates neuropathic and visceral pain in mice. *Neuropharmacology* **138**, 232-244 (2018).
41. Coen, N., Duraffour, S., Snoeck, R. & Andrei, G. KSHV Targeted Therapy: An Update on Inhibitors of Viral Lytic Replication. *Viruses* **6**(2014).
42. Rohner, E.*, et al.* HHV-8 seroprevalence: a global view. *Systematic Reviews* **3**, 11 (2014).

bioRxiv preprint doi: https://doi.org/10.1101/2021.09.10.459757; this version posted September 10, 2021. The copyright holder for this preprint (which was not certified by peer review) is the author/funder. All rights reserved. No reuse allowed without permission.

43. King, J.T., Justice, A.C., Roberts, M.S., Chang, C.-C.H. & Fusco, J.S. Long-Term HIV/AIDS Survival Estimation in the Highly Active Antiretroviral Therapy Era. *Medical Decision Making* **23**, 9-20 (2003).
44. Scott, C. & Griffin, S. Viroporins: structure, function and potential as antiviral targets.
45. Teisseyre, A., Palko-Labuz, A., Sroda-Pomianek, K. & Michalak, K. Voltage-Gated Potassium Channel Kv1.3 as a Target in Therapy of Cancer. *Front Oncol* **9**, 933 (2019).
46. Bajaj, S. & Han, J. Venom-Derived Peptide Modulators of Cation-Selective Channels: Friend, Foe or Frenemy. *Frontiers in Pharmacology* **10**, 58 (2019).
47. Pennington, M.W.*, et al.* Development of highly selective Kv1.3-blocking peptides based on the sea anemone peptide ShK. *Mar Drugs* **13**, 529-542 (2015).
48. Uldrick, T.S.*, et al.* Rituximab plus liposomal doxorubicin in HIV-infected patients with KSHV-associated multicentric Castleman disease. *Blood* **124**, 3544-3552 (2014).
49. Frishman, W.H. Mibefradil: A New Selective T-Channel Calcium Antagonist for Hypertension and Angina Pectoris.
50. Mankouri, J.*, et al.* Suppression of a pro-apoptotic K⁺ channel as a mechanism for hepatitis C virus persistence. *Proceedings of the National Academy of Sciences* **106**, 15903 (2009).
51. Dobson, S.J., Mankouri, J. & Whitehouse, A. Identification of potassium and calcium channel inhibitors as modulators of polyomavirus endosomal trafficking. *Antiviral Research* **179**, 104819 (2020).
52. Tarcha, E.J.*, et al.* Safety and pharmacodynamics of dalazatide, a Kv1.3 channel inhibitor, in the treatment of plaque psoriasis: A randomized phase 1b trial. *PLOS ONE* **12**, e0180762 (2017).

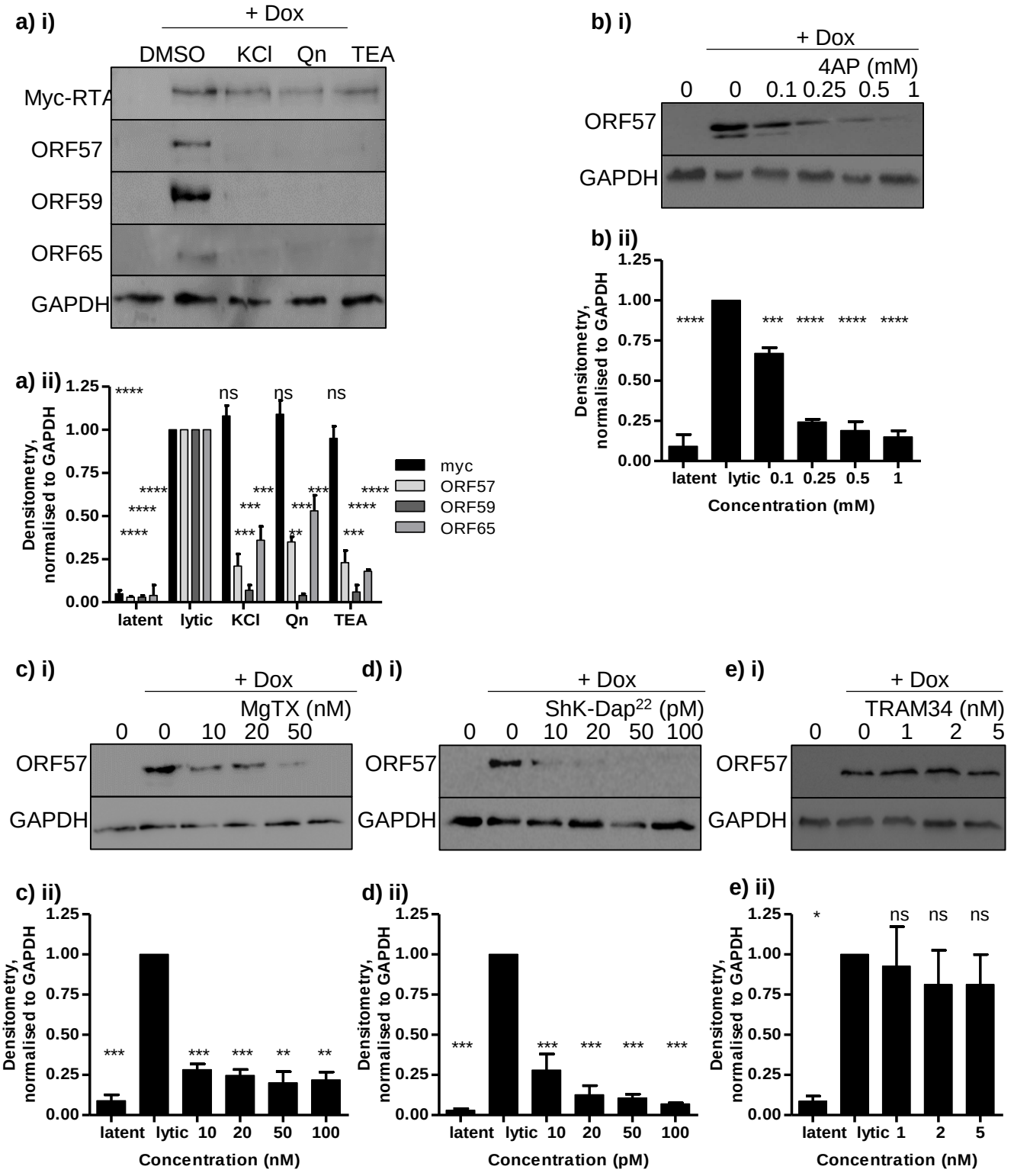

Figure 1. K+ channels are required for efficient KSHV lytic replication.

TREx BCBL1-RTA cells remained unreactivated or were pre-treated with non-cytotoxic concentrations of (A) general K^+ inhibitors, 25 mM KCl, 100 µM Qn and 10 mM TEA, , or increasing amounts of (B) 4AP (C) MgTX, (D) ShK-Dap^{22} and (E) TRAM34 for 45 minutes prior to reactivation with doxycycline hyclate for 48 hr. (i) Cell lysates were then probed with ORF57-, ORF59- or ORF65-specific antibodies. GAPDH was used as a measure of equal loading (ii) Densitometry quantification of immunoblots was carried out using the Image J software and is shown as a percentage relative to the loading control, GAPDH. Data analysed using three replicates per experiment, n = 3 and statistical analysis using a two-tailed t-test with unequal variance, ** = $p<0.01$, **** = $p<0.001$, **** = $p<0.0001$.

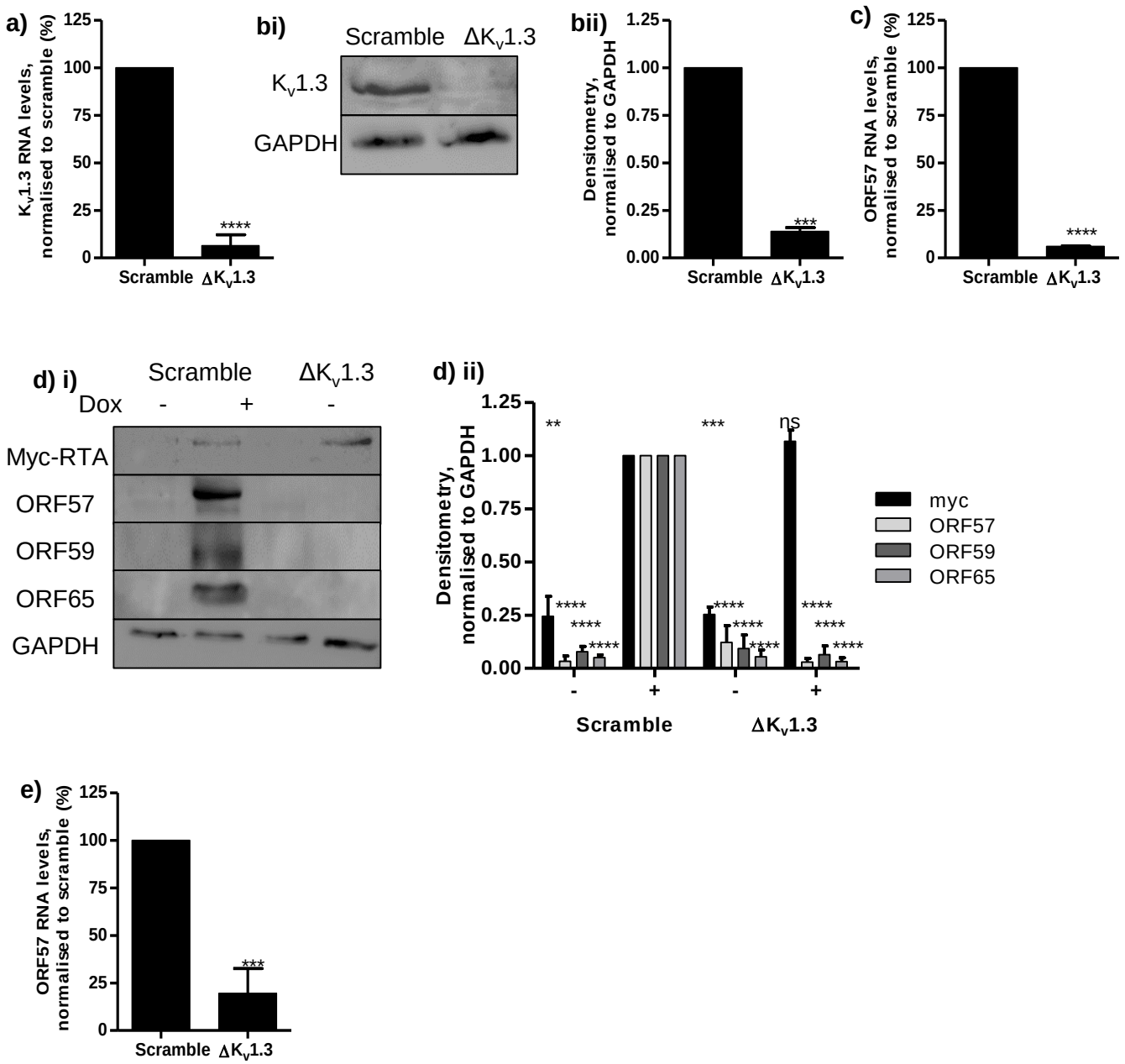

Figure 2. K_v1.3 is required for efficient KSHV lytic replication.

TREx BCBL1-RTA cells were stably transduced with lentivirus expressing scrambled or K_v1.3-specfic shRNAs. Scramble and K_v1.3-depleted cells lines were reactivated with doxycycline hyclate for 24 hr. (A) Total RNA was extracted and relative transcript levels were analysed by qRT-PCR using GAPDH as a reference. Fold change was determined by ΔΔCt and statistical significance analysed using a non-paired t-test, **** = p<0.0001. B and C (i) Cell lysates were probed with (B) K_v1.3- or (C) ORF57-, ORF59- or ORF65-specific antibodies and GAPDH used as a measure of equal loading (ii) Densitometry quantification of immunoblots was carried out using the Image J software and is shown as a percentage relative to the loading control, GAPDH. Data analysed using three replicates per experiment, n = 3 and statistical analysis using a two-tailed t-test with unequal variance, *** = p<0.001, **** = p<0.0001. (D) Scramble or K_v1.3-depletetd TREx BCBL1-RTA cells were reactivated for 72 h. The culture medium was then incubated for 24 h with HEK-293T cells followed by total RNA extraction and qRT-PCR. Results show the mean of three biological replicates with error bar as standard deviation, *** = p<0.001.

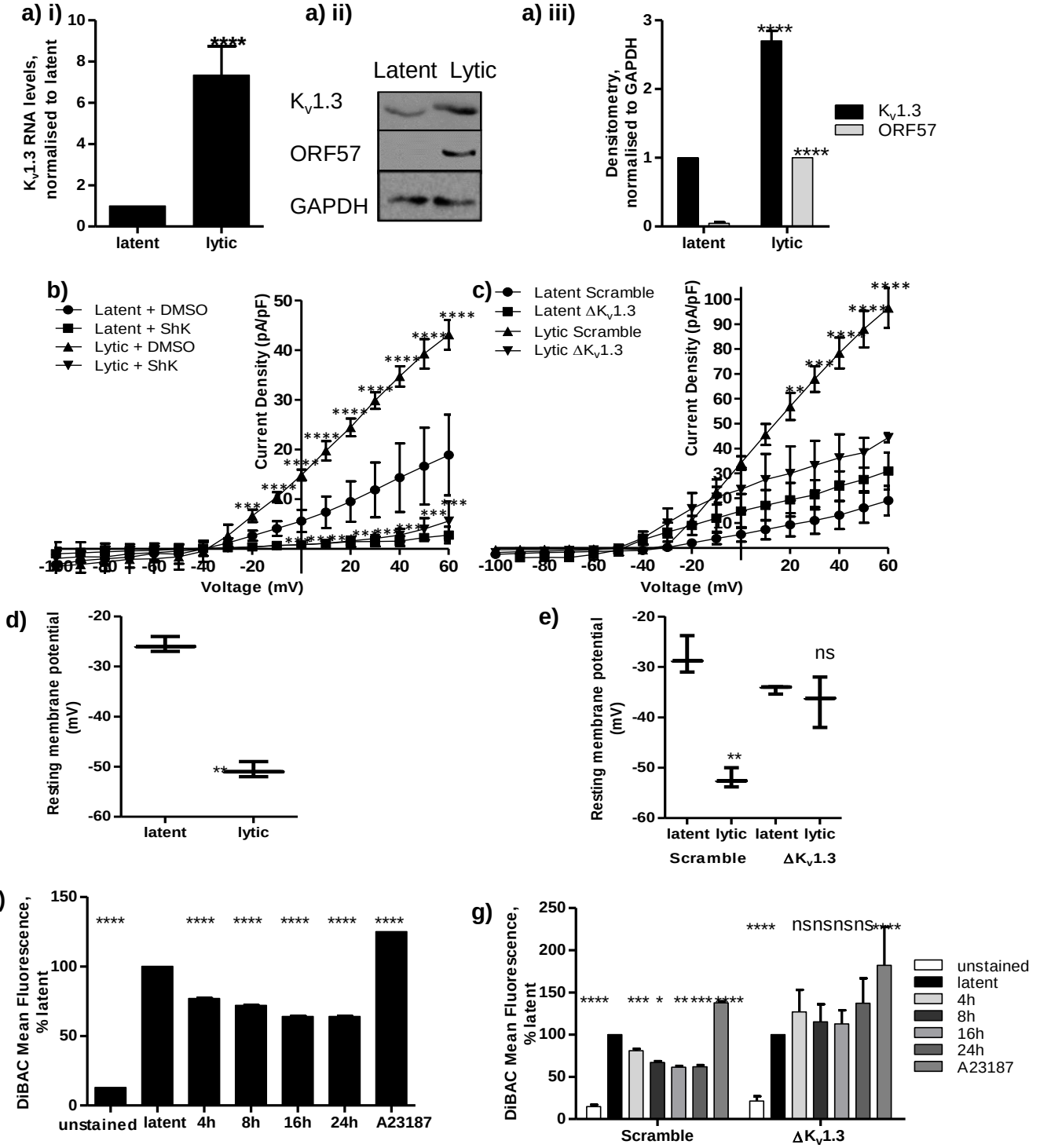

Figure. 3. Increased K_v1.3 currents during lytic KSHV replication.

(A) TREx BCBL1-RTA cells remained unreactivated or were reactivated with doxycycline hyclate for 24 hr. (i) Total RNA was extracted and relative K_v1.3 transcript levels were analysed by qRT-PCR using GAPDH as a reference. Fold change was determined by ΔΔCt and statistical significance analysed using a non-paired t-test, **** = p<0.0001. (ii) Cell lysates were probed with K_v1.3-specific antibodies and GAPDH used as a measure of equal loading (iii) Densitometry quantification of immunoblots was carried out using the Image J software and is shown as a percentage relative to the loading control, GAPDH. Data analysed using three replicates per experiment, n = 3 and statistical analysis using a two-tailed t-test with unequal variance, *** = p<0.001, **** = p<0.0001. Mean current density voltage relationships for K^+ currents (n=5 for all populations) from (B) unreactivated and reactivated TREx BCBL1-RTA at 16 hr; cells were pre-treated for 24 hours with DMSO control or 100 pM ShK-Dap^{22} and (C) Scramble and K_v1.3-depleted cells lines which remained unreactivated or were reactivated with doxycycline hyclate for 24 hr. Pooled data highlighting resting membrane potentials in (D) latent and lytic TREx BCBL1-RTA cells or (E) Scramble and K_v1.3-depleted cells lines. Membrane polarisation of TREx BCBL1-RTA cells was measured by Flow cytometry after a 5 min incubation with DiBAC4(3) (F) Unreactivated and reactivated TREx BCBL1-RTA at 24 hr or (G) Scramble and K_v1.3-depleted cells lines.

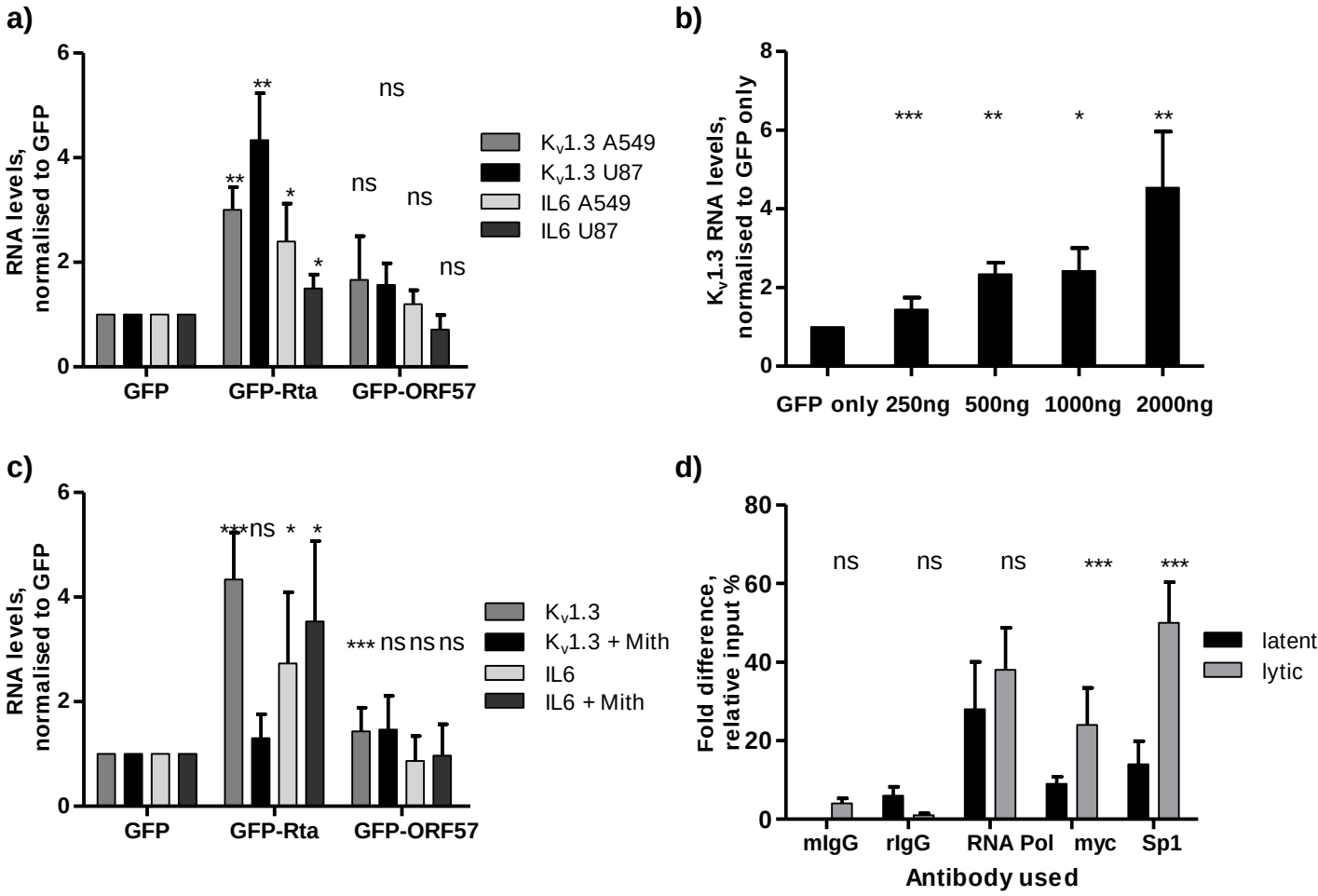

Figure 4 KSHV RTA upregulates K_v1.3 expression.

A549 and U87 cells were transfected with either (A) GFP, RTA-GFP or ORF57–GFP expression construct for 24 hr, (B) Dose-dependent increase of RTA-GFP for 24 hr or (C) GFP, RTA-GFP or ORF57–GFP in the presence of the Sp1 inhibitor, Mithramycin A. Total RNA was extracted and relative K_v1.3 or IL-6 transcript levels were analysed by qRT-PCR using GAPDH as a reference. Fold change was determined by ΔΔCt and statistical significance analysed using a non-paired t-test, * = p<0.05, ** = p<0.01, *** = p<0.001. (D) ChIP assays were carried out on unreactivated versus reactivated TREx BCBL1-RTA cells using antibodies specific to SP-1, RNAPII, myc-RTA or mouse and rabbit IgG control antibodies. PCR amplification was carried out on the immunoprecipitates using primers against the K_v1.3 promoter region to determine association. The average of three independent experiments is shown with error bars as standard deviation, *** = p<0.001.

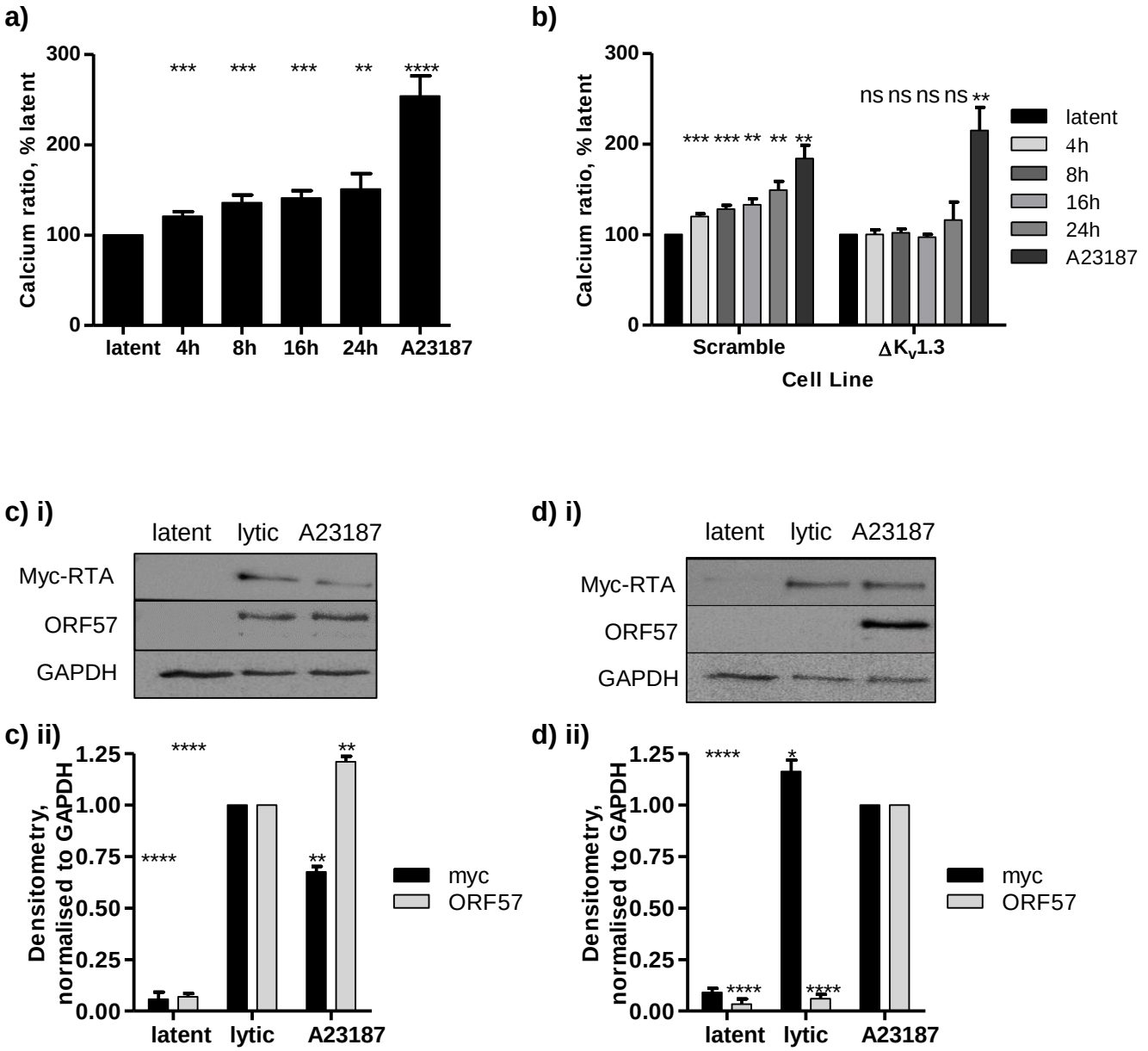

Figure 5. Membrane hyperpolarisation leads to Ca^{2+} influx during KSHV lytic replication.

Fura Red staining of calcium ratios were measured in TREx BCBL1-RTA cells by Flow cytometry, the calcium ionophore A23187 was used as a positive control (A) Unreactivated and reactivated TREx BCBL1-RTA at 24 hr or (B) Scramble and K_v1.3-depleted cells lines. (C) Unreactivated and reactivated TREx BCBL1-RTA at 24 hr or (D) Scramble and K_v1.3-depleted cells lines were assessed for levels of lytic replication in the presence of the calcium ionophore A2318, (i) Cell lysates were probed with ORF57-specific antibodies and GAPDH used as a measure of equal loading (ii) Densitometry quantification of immunoblots was carried out using the Image J software and is shown as a percentage relative to the loading control, GAPDH. Data analysed using three replicates per experiment, n = 3 and statistical analysis using a two-tailed t-test with unequal variance, *** = $p<0.001$, **** = $p<0.0001$.

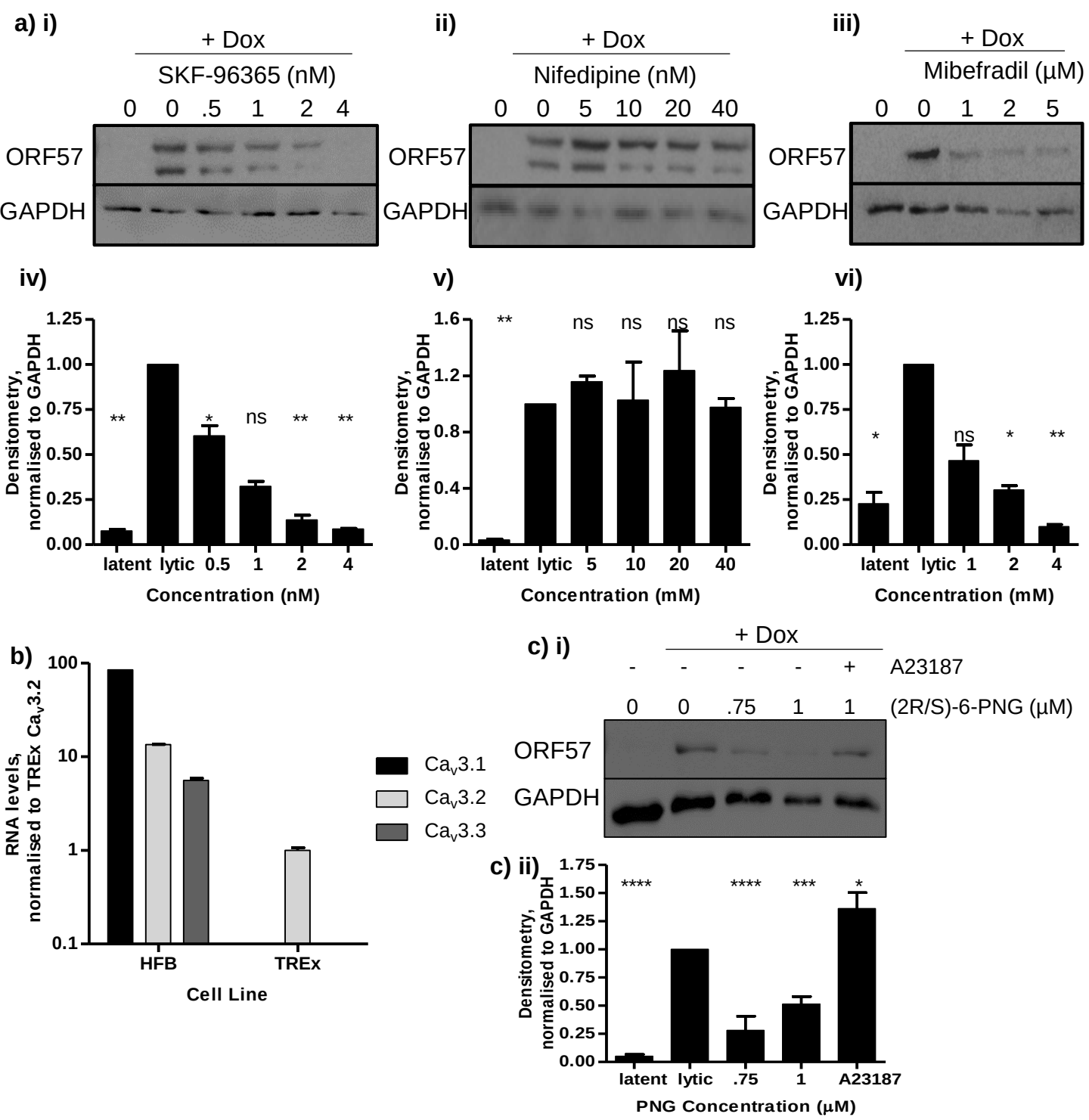

Figure 6 KSHV-mediated calcium influx requires the T-type voltage-gated calcium channel, $Ca_v3.2$.

(A) TREx BCBL1-RTA cells remained unreactivated or were pre-treated with non-cytotoxic dose-dependent concentrations of Ca^{2+} channel inhibitors, (i) T-type and TRP channel inhibitor, SKF-96365 (ii) L-type voltage-gated inhibitor, nifedipine and (iii) T-type inhibitor, mibefradil for 45 minutes prior to reactivation with doxycycline hyclate for 48 hr. Cell lysates were then probed with ORF57-specific antibodies. GAPDH was used as a measure of equal loading. (iv-vi) Densitometry quantification of immunoblots was carried out using the Image J software and is shown as a percentage relative to the loading control, GAPDH. Data analysed using three replicates per experiment, n = 3 and statistical analysis using a two-tailed t-test with unequal variance, * = p<0.01, ** = p<0.001. (B) T-type Ca^{2+} channel expression was analysed by qRT-PCR from total RNA was extracted from latent TREx BCBL1-RTA, and Human foetal brain cDNA using GAPDH as a reference. (C) (i) TREx BCBL1-RTA cells remained unreactivated or were pre-treated with non-cytotoxic dose-dependent concentrations of 2R/S-6-PNG for 45 minutes prior to reactivation. Cell lysates were probed with ORF57-specific antibodies. GAPDH was used as a measure of equal loading. (ii) Densitometry quantification of immunoblots was carried out using the Image J software and is shown as a percentage relative to the loading control, GAPDH. Data analysed using three replicates per experiment, n = 3 and statistical analysis using a two-tailed t-test with unequal variance, *** = p<0.001, **** = p<0.0001.

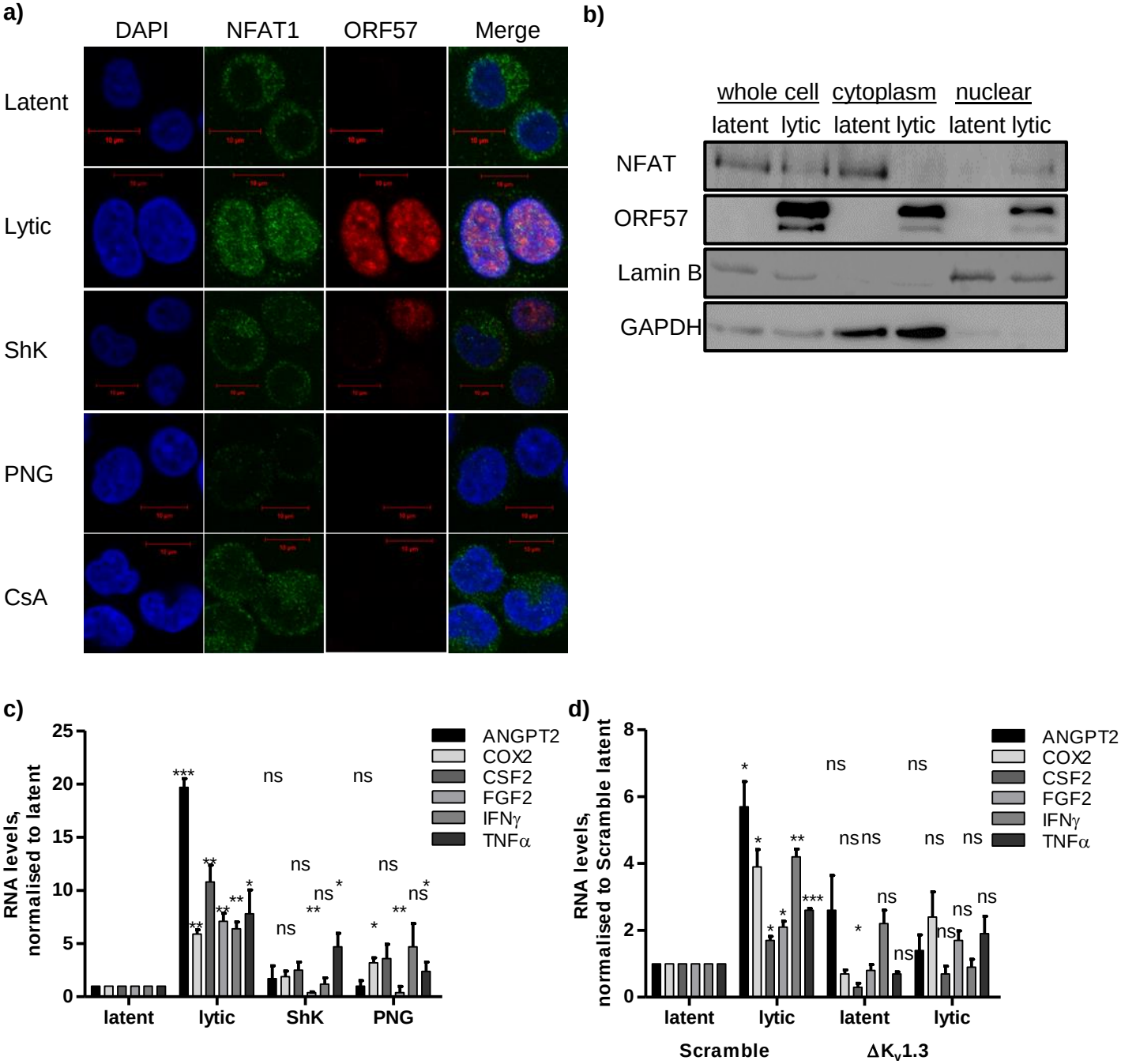

Figure 7. KSHV-mediated calcium influx initiates NFAT1 nuclear localisation and NFAT1-mediated gene expression.

(A) TREx BCBL1-RTA cells remained unreactivated or were pre-treated with inhibitors for 45 minutes prior to reactivation with doxycycline hyclate for 24 hr. Endogenous NFAT1 and ORF57 proteins were identified by indirect immunofluorescence using specific antibodies. (B) Cells were harvested from latent and reactivated TREx BCBL1-RTA cells at 24 hr and subcellular fractions were probed with ORF57- and NFAT-specific antibodies, GAPH and Lamin B were used as a measure of equal loading and purity of fractions. Total RNA was extracted from (C) unreactivated and reactivated TREx BCBL1-RTA cells at 24 hr, or cells pre-treated with ShK-Dap[22] or PNG and (D) Scramble and K_v1.3-depleted cells lines which remained unreactivated or were reactivated with doxycycline hyclate for 24 hr. Relative NFAT-responsive transcript levels were analysed by qRT-PCR using GAPDH as a reference. Fold change was determined by ΔΔCt and statistical significance analysed using a non-paired t-test, * = p<0.05, ** = p<0.01, *** = p<0.001.

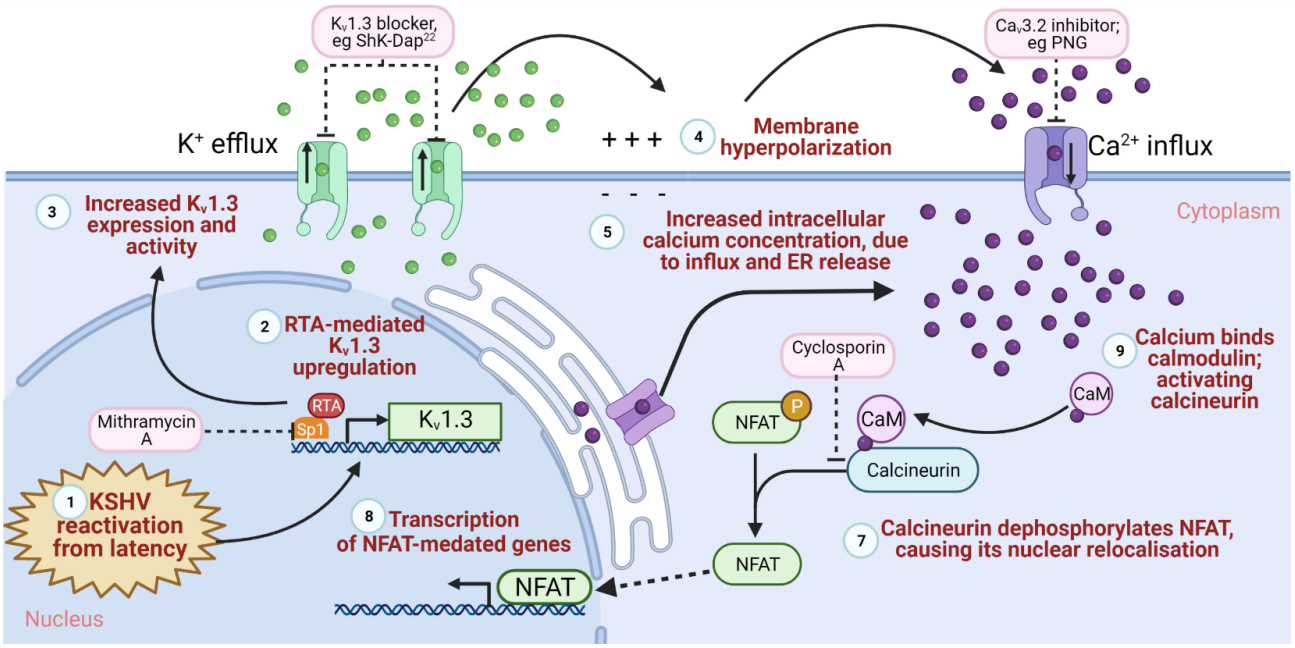

Figure 8. A K_v1.3-Ca_v3.2 axis is a direct contributor to KSHV lytic replication in B cells.
Schematic representation of the KSHV-mediated K_v1.3 induced hyperpolarisation and Ca_v3.2-mediated calcium entry mechanism required for efficient lytic replication. Potential therapeutic interventions are highlighted. Created with Biorender.com